

Relativistic effects on the structural phase stability of molybdenum

This article has been downloaded from IOPscience. Please scroll down to see the full text article.

1999 J. Phys.: Condens. Matter 11 3237

(<http://iopscience.iop.org/0953-8984/11/16/005>)

View [the table of contents for this issue](#), or go to the [journal homepage](#) for more

Download details:

IP Address: 171.66.16.214

The article was downloaded on 15/05/2010 at 07:19

Please note that [terms and conditions apply](#).

Relativistic effects on the structural phase stability of molybdenum

J C Boettger

Theoretical Division, Los Alamos National Laboratory, Los Alamos, NM 87545, USA

Received 12 January 1999

Abstract. The relative stabilities of the fcc, bcc, and hcp structures of molybdenum (Mo) are studied as functions of volume with both nonrelativistic and scalar-relativistic linear combinations of Gaussian-type orbitals (LCGTO) fitting function calculations. Relativity is shown to have a significant effect on the bcc–fcc structural energy difference that first increases, then decreases, with pressure, but has only a negligible effect on the hcp–fcc structural energy difference. The scalar-relativistic bcc–fcc energy difference curve obtained here is in good agreement with an earlier fully relativistic calculation using the all-electron full-potential linear muffin-tin orbital method. Unlike previous theoretical work, this investigation finds no region of hcp phase stability at $T = 0$. Instead, the bcc phase transforms directly into the fcc phase at a pressure of about 6.6 Mbar.

1. Introduction

The linear combinations of Gaussian-type orbitals (LCGTO) technique is the most widely used electronic structure method in existence today. The great popularity of the LCGTO method is a natural consequence of its wide range of applicability and its conceptual simplicity. Since GTO basis functions are short ranged and atom centred, the LCGTO method is applicable to any multi-atom system, regardless of spatial symmetry. Thus, the LCGTO method is able to treat isolated clusters of atoms, polymer chains, thin films, and crystalline solids on an equal footing—thereby bridging the often wide gap between solid-state physics and quantum chemistry. The simple form of the GTO basis functions allows all four-centre Coulomb integrals to be calculated analytically, making it possible to carry out LCGTO calculations using density functional theory (DFT), Hartree–Fock theory (with or without correlation), or some mixture of the two (the hybrid method). Finally, the fact that GTOs are exponentially local in both real and reciprocal space makes them attractive candidates for basis functions to be used in linear scaling methods. Thus, the LCGTO method may be viewed, to some extent, as a ‘universal’ electronic structure methodology.

One long-standing disadvantage of the LCGTO technique relative to the numerical-orbital-based DFT electronic structure techniques often employed in solid-state physics, such as the full-potential linear augmented-plane-wave (FLAPW) method and the full-potential linear muffin-tin orbital (FLMTO) method, has been the lack of a stable technique for incorporating relativistic effects during all-electron calculations on systems that include heavy atoms—an affliction shared by most fixed-basis-set methods [1]. This limitation effectively restricts all-electron LCGTO calculations to systems formed from atoms in the first three rows of the periodic table—i.e., less than half of all atoms. Although a number of strategies have been suggested for incorporating relativistic effects into fixed-basis-set calculations [1], most

practical LCGTO calculations for heavy-atom systems still rely on some form of relativistic pseudopotential.

In recent years, considerable progress has been made toward developing a computationally tractable relativistic LCGTO method. One particularly fruitful line of research has been based on the so-called Douglas–Kroll–Hess [2–4] (DKH) transformation. As early as 1986, B A Hess was carrying out scalar-relativistic LCGTO Hartree–Fock calculations on molecular systems [3]. A few years later, Häberlen and Rösch [5] demonstrated the feasibility of carrying out scalar-relativistic LCGTO DFT calculations on heavy-atom clusters using a simplified ‘incomplete’ DKH transformation. In 1997, Geipel and Hess [6] published the first all-electron, scalar-relativistic, Hartree–Fock LCGTO calculation for a crystalline solid, using a modified version of the program CRYSTAL88 [7]. The first scalar-relativistic DFT LCGTO calculation for a solid was published the next year [8], using the LCGTO fitting function (LCGTO-FF) method [9, 10], as implemented in the program GTOFF [11]. These developments have established the all-electron, scalar-relativistic LCGTO method, based on the DKH transformation, as a viable technique for studying local and extended heavy-atom systems utilizing either Hartree–Fock or DFT theory—or, by extension, hybrid methods.

In the present work, the new scalar-relativistic version of GTOFF [8] is used to study the effect of relativity on the equation of state and structural phase stability of Mo. Since Mo is a standard test case for crystalline electronic structure techniques, numerous calculations of its zero-pressure properties [12–18], both relativistic and nonrelativistic, are available for comparison. In addition, the structural phase stability of Mo has been studied with at least one high-precision, all-electron, relativistic DFT technique: the full-potential linear muffin-tin orbital (FLMTO) method [19]. Thus the current investigation provides an important test of the scalar-relativistic LCGTO-FF method on a rather subtle relativistic effect [20].

The scalar-relativistic LCGTO-FF method will be reviewed in the following section. In the third section, the basis sets used here and a few other computational details will be discussed. The results obtained here for the zero-pressure properties, equation of state, and structural phase stability of Mo will be presented and compared with previous calculations in the fourth section. A few concluding remarks will be given in the final section.

2. The scalar-relativistic LCGTO method

The development of the scalar-relativistic LCGTO-FF method used here begins with the four-component Dirac–Kohn–Sham (DKS) equations [21]:

$$h_{DKS}^{(4)}\psi_i = [(c\boldsymbol{\alpha} \cdot \mathbf{p} + \beta mc^2) + v_{eff}] \psi_i = \epsilon_i \psi_i \quad (1)$$

where

$$v_{eff} = v_n + v_c + v_{xc} \quad (2)$$

is the effective one-electron potential formed from the nuclear potential v_n , the classical electronic Coulomb potential v_c , and the DFT exchange–correlation (XC) potential v_{xc} . The eigenvalues of the DKS equations are unbounded, above and below, since they include both electron and positron degrees of freedom. Therefore, any attempt to solve the DKS equations variationally will lead to the ‘variational collapse’ problem, unless the freedom of the basis set used is carefully restricted [1]. (For example, solid-state electronic structure techniques like the FLAPW and FLMTO methods use numerical basis functions that are constructed to be electronic solutions for a muffin-tin potential, effectively restricting the variational freedom of the basis.) The variational collapse problem can also be circumvented by performing some unitary transformation on the DKS equations that approximately decouples the electron

and positron degrees of freedom. For example, it is well known that the DKS equations can be decoupled to arbitrary order in $(\mathbf{p}/mc)^2$ via a series of Foldy–Wouthuysen [22] transformations. Unfortunately, the Foldy–Wouthuysen procedure produces operators that are highly singular at the nucleus, and are hence not amenable to an all-electron variational solution.

An alternative approach, which does not generate singular operators, uses the DKH transformation [2–4] to decouple the DKS equations to second order in the external field, v_{eff} . This procedure yields the two-component, external-field projector (EFP) equation:

$$\begin{aligned} h_{EFP}^{(2)}\phi_i &= \epsilon_i\phi_i \\ h_{EFP}^{(2)} &= E_p + A_p [v_{eff} + R_p v_{eff} R_p] A_p - \frac{1}{2}(E_p W^2 + W^2 E_p + 2W E_p W) \end{aligned} \quad (3)$$

where

$$E_p = c(p^2 + m^2c^2)^{1/2}. \quad (4)$$

Also,

$$A_p = \left[\frac{E_p + mc^2}{2E_p} \right]^{1/2} \quad (5)$$

$$R_p = K_p \boldsymbol{\sigma} \cdot \mathbf{p} \quad (6)$$

$$K_p = c/(E_p + mc^2) \quad (7)$$

and W can be expressed in momentum space as

$$W_{p,p'} = A_p(R_p - R_{p'})A_{p'} \left[\frac{v_{eff}(\mathbf{p}, \mathbf{p}')}{E_p + E_{p'}} \right] \quad (8)$$

where $v_{eff}(\mathbf{p}, \mathbf{p}')$ is the momentum-space representation of v_{eff} . As written, the EFP equations are fully relativistic, in the sense that they include mass–velocity, Darwin, and spin–orbit coupling corrections. Throughout the remainder of this work, it will be assumed that all of the spin–orbit coupling terms in equation (3) are neglected to obtain the scalar-relativistic EFP approximation. (A detailed discussion of the separation of the relativistic corrections into scalar-relativistic and spin–orbit coupling terms has been presented elsewhere [23] and will not be repeated here.)

Analytical evaluation of the GTO matrix elements for the momentum-space operators in equation (3) has not proven to be practical thus far. This difficulty can be circumvented by using an approximate momentum-space representation obtained by diagonalizing the nonrelativistic kinetic-energy matrix [24]. First, the matrix elements of $\mathbf{p} \cdot \mathbf{v}\mathbf{p}$ and $\mathbf{p} \times \mathbf{v}\mathbf{p}$ (which are required even for scalar-relativistic EFP calculations) are evaluated along with the usual nonrelativistic matrix elements. Next, the nonrelativistic kinetic-energy matrix is diagonalized to obtain approximate eigenfunctions of p^2 and all of the matrices are transformed to this approximate momentum space. Since the operators E_p , A_p , and K_p are diagonal in momentum space, they can be obtained trivially from the p^2 -eigenvalues. These basic components are then used to build the more complicated matrix elements needed, such as $A_p R_p v R_p A_p$. Finally, all of the matrices are back-transformed to the original GTO representation.

The most serious drawback to the procedure described above is the fact that the relativistic corrections to the two-electron and exchange–correlation integrals are very demanding computationally. Fortunately, these corrections are quite small and can be neglected in most practical calculations [5, 6, 8]; this is the nuclear-only approximation. Häberlen and Rösch [5] achieve a further reduction in the resources required for their calculations by dropping all terms in the nuclear-only EFP equation that require $\mathbf{p} \times v_n \mathbf{p}$; this is the HR approximation. A recent

series of test calculations on isolated atoms [23] found that the HR approximation produces one-electron eigenvalues for the chemically active valence states that differ little from those obtained with the complete scalar-relativistic Douglas–Kroll–Hess transformation. This then is the version of scalar relativity implemented in GTOFF.

The nuclear-only approximation introduces one additional difficulty that is unique to extended system calculations. Solid-state electronic structure codes typically make use of charge neutrality to ensure that the Coulomb lattice sums converge, a constraint that is not satisfied for the relativistic corrections to the nuclear-only Coulomb integrals. Geipel and Hess [6] resolve this difficulty by taking advantage of the anticipated short range of the relativistic corrections; i.e., they simply carry out the lattice sums over a fixed number of neighbour sites and assume that the correction terms will be converged. GTOFF uses a different approach that explicitly includes the long-range contributions to the corrections and converges all of the lattice sums. This is accomplished by making use of the fact that the contributions of $v_{eff}(\mathbf{0}, \mathbf{0})$ to the relativistic corrections in equation (3) cancel exactly. Thus, the relativistic corrections can be obtained by embedding the nuclear lattice in a neutralizing, uniform electron gas and then using a generalized Ewald procedure to calculate the lattice sums to high precision.

3. Computational details

The LCGTO-FF technique is distinguished from other electronic structure methods by its use of three independent GTO basis sets to expand the orbitals, charge density, and local density approximation (LDA) exchange–correlation (XC) integral kernels—here using the LDA parametrization of Hedin and Lundqvist (HL) [25]. The charge fitting functions are used to reduce the total number of Coulomb integrals by replacing the usual four-centre integrals in the total-energy and one-electron equations with three-centre integrals. The charge fitting function coefficients are determined by minimizing the error in the Coulomb energy due to the fit [26]; this allows high-precision calculations with relatively small basis sets. The least squares XC fit used here acts as a simple yet sophisticated numerical quadrature scheme capable of producing accurate results with a rather coarse numerical integration mesh. The precision of any LCGTO-FF calculation will, of course, be largely determined by the selection of these three basis sets.

The orbital basis set used here for volumes near ambient was derived from Huzinaga's 17s11p8d atomic basis [27] by replacing the five most diffuse s-type GTOs with more local basis functions, augmenting the p-type basis with one diffuse GTO, and adding two f-type polarization functions. The resulting 17s12p8d2f crystalline basis set was then reduced to a 13s8p5d2f basis set by contracting the most local GTOs of each *l*-type using atomic orbital coefficients from nonrelativistic or scalar-relativistic atomic calculations. The charge density and the XC integral kernels were fitted with a single 15s GTO basis set, selected on the basis of prior experience with LCGTO-FF calculations. The orbital and fitting function exponents used near the ambient volume of Mo have been listed elsewhere [20], with the exception of the f-type orbital exponents, 1.1 and 0.5, which were not used in the earlier work. For the more highly compressed volumes considered here, the exponents of the most diffuse GTOs were increased as needed to avoid numerical instabilities due to near linear dependencies. In all cases, the same basis sets were used for a given volume regardless of the crystal structure under consideration.

All Brillouin zone (BZ) integrations were carried out on a uniform mesh with 145 (150) irreducible *k*-points for the cubic (hexagonal) structures, using a Gaussian broadened (10 mRyd) histogram integration technique. Additional calculations using a sparser mesh with 72 (73) irreducible *k*-points indicate that the calculations are well converged with respect

to the mesh density. The SCF cycle was iterated until the total energy varied by less than 0.004 mRyd/atom.

4. Results

Nonrelativistic and scalar-relativistic total energies were calculated for fcc, bcc, and hcp Mo at ten volumes ranging from 41.8414 au to 113.4905 au. Cohesive energies were obtained by removing atomic energies calculated in a manner consistent with the crystalline calculations. (For the atomic calculations, the basis sets were augmented with diffuse functions to mimic the effect of off-site functions on the crystalline calculations.) The resulting cohesive energies are listed in table 1.

Table 1. Nonrelativistic and scalar-relativistic cohesive energies (Ryd) for fcc, bcc, and hcp Mo at ten volumes (au).

V	fcc	bcc	hcp
Nonrelativistic			
113.4905	-0.503292	-0.531374	-0.500422
108.0000	-0.508402	-0.537694	-0.505725
102.6895	-0.509338	-0.539726	-0.506953
97.5560	-0.505538	-0.536576	-0.503422
92.5965	-0.496454	-0.527502	-0.494297
83.5965	-0.460694	-0.490426	-0.458470
73.1399	-0.371734	-0.396196	-0.369888
62.6877	-0.195846	-0.206556	-0.193548
52.2768	0.137562	0.152764	0.143635
41.8414	0.811176	0.857810	0.819401
Scalar relativistic			
113.4905	-0.544010	-0.573812	-0.539869
108.0000	-0.550128	-0.581482	-0.546135
102.6895	-0.551964	-0.584798	-0.548202
97.5560	-0.548858	-0.582910	-0.545398
92.5965	-0.540066	-0.575076	-0.536910
83.5965	-0.504112	-0.539442	-0.501418
73.1399	-0.414154	-0.445640	-0.411685
62.6877	-0.235102	-0.256252	-0.232892
52.2768	0.106946	0.110726	0.112138
41.8414	0.791936	0.829298	0.801422

The zero-pressure properties for each structure were obtained by fitting the cohesive energies for the six largest volumes in table 1 with a modified version of the universal equation of state [28]. Table 2 compares the lattice constant a_0 , bulk modulus B , and pressure derivative of the bulk modulus B' found here both nonrelativistically and scalar relativistically, with results from a number of other calculations. Experimental room temperature values [29] for a_0 , B , and B' are listed in table 2 for the bcc structure. A 20 K value is also listed for a_0 to allow a better comparison with the static-lattice theoretical values [30].

Although the zero-pressure properties obtained here are generally consistent with previous results, the lattice constants are slightly smaller and the bulk moduli are a bit larger. The reduced lattice constants can be attributed to the very rich basis sets being used here, which will tend to strengthen the bonding, while the increase in the bulk modulus is a natural consequence of the reduced lattice constant. Certainly, the lattice constant reduction and

Table 2. Lattice constants (a_0 ; Bohr), bulk moduli (B ; GPa), and pressure derivatives of the bulk moduli (B') for hcp, fcc, and bcc Mo obtained here from nonrelativistic (N) and relativistic (R) LCGTO-FF calculations are compared with other calculations and experiment. The hcp results were obtained for an ideal c/a ratio.

Method	N/R	Structure	Reference	a_0	B	B'
LCGTO-FF	N	hcp	Present	5.276	254	3.97
LCGTO-FF	R	hcp	Present	5.261	268	4.09
LCGTO-FF	N	fcc	Present	7.468	250	3.91
LAPW	R	fcc	13	7.504	247	
APW	R	fcc	16	7.475	256	
LCGTO-FF	R	fcc	Present	7.446	269	3.93
KKR	N	bcc	12	5.91	251	
FLMTO	N	bcc	14	5.97	255	
LMTO-ASA	N	bcc	15	5.948	265	4.38
LCGTO-FF	N	bcc	Present	5.909	279	3.95
LAPW	R	bcc	13	5.917	291	
LMTO-ASA	R	bcc	15	5.910	248	4.99
APW	R	bcc	16	5.904	288	
FLMTO	R	bcc	17	5.879	297	
FCD-LMTO	R	bcc	18	5.906	306	
LCGTO-FF	R	bcc	Present	5.883	293	4.19
Experiment: 300 K		bcc	29	5.948	261	4.46
Experiment: 20 K		bcc	30	5.943		

bulk modulus enhancement relative to experiment are no larger than would be expected for an LDA calculation. The theoretical results in table 2 are also consistent with the widely held belief that relativistic effects are quite small for d-bonded materials, making it difficult to judge the overall reliability of the scalar-relativistic LCGTO-FF method on the basis of the zero-pressure properties of Mo. Still, the relativistic shift found here for the lattice constant of bcc Mo (-0.026 au) is in reasonable agreement with the -0.038 au shift found by Moriarty [15] using the more approximate LMTO-ASA method.

Figure 1 compares the nonrelativistic and scalar-relativistic bcc–fcc and hcp–fcc structural energy differences found here with energy differences determined from fully relativistic FLMTO calculations [19]. Figure 1 reveals four important results:

- relativity has a significant effect on the bcc–fcc structural energy difference that initially increases with pressure;
- the scalar-relativistic LCGTO-FF results for the bcc–fcc structural energy differences are in good agreement with the earlier FLMTO results, demonstrating the ability of the LCGTO-FF method to resolve a subtle, but important, relativistic effect;
- the effect of relativity on the hcp–fcc structural energy difference is negligible; and
- the LCGTO-FF and FLMTO results for the hcp–fcc energy difference curves disagree, with the FLMTO results predicting a small region of hcp stability at $T = 0$ and the LCGTO-FF results indicating that there is no region of hcp stability.

The disagreement between the FLMTO and LCGTO-FF results for the hcp–fcc structural energy difference is an obvious cause for concern and will be addressed first. Since relativity has little effect on the hcp–fcc energy differences, some other source for the disagreement must be found. The most obvious candidate is the large difference between the orbital basis sets used for the two calculations. In particular, whereas the LCGTO-FF calculations included s-, p-, d-, and f-type basis functions, the FLMTO calculations only utilized s-, p-, and d-type

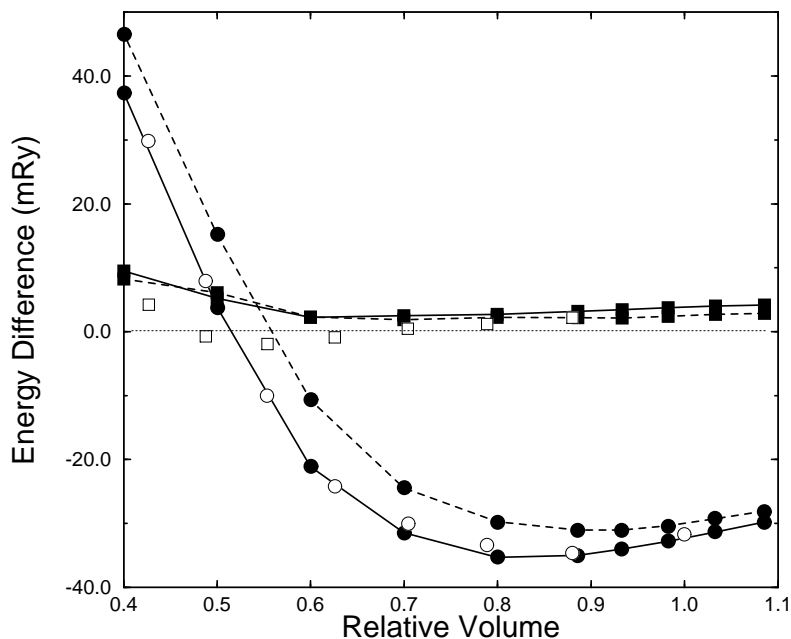


Figure 1. The bcc–fcc (circles) and hcp–fcc (squares) structural energy differences for Mo obtained here with scalar-relativistic (solid curve) and nonrelativistic (dashed curve) LCGTO-FF calculations are compared with FLMTO results (open symbols) from reference [19]. The reference volume is 104.951 au.

basis functions. Since the hcp structure is the only structure considered here that does not have inversion symmetry at the atomic sites, it might respond differently to the inclusion of *f*-type functions. To test this conjecture, P Söderlind [31] has carried out a set of FLMTO calculations for fcc and hcp Mo, with *f*-type basis functions included. Those calculations indicate that there is no region of hcp stability at $T = 0$ K, in good qualitative agreement with the present results. It should be noted however that the hcp–fcc structural energy differences are too small to entirely rule out the possibility of hcp Mo, especially if relaxation of the c/a ratio were allowed.

Although the relativistic correction to the bcc–fcc structural energy difference is fairly small, it significantly delays the onset of the bcc \rightarrow fcc phase transition from a relative volume of about 0.55 to roughly 0.51. This delay in the transition has a rather simple interpretation. It is well known that pressure-induced structural phase transitions are frequently associated with a transfer of electrons from states of low angular momentum to states with higher angular momentum. For example, elemental solids formed from third-row atoms exhibit phase transitions that can be related to a pressure-induced transfer of electrons from the 3s state to the 3d state [32]. Since it is also well established that relativity reduces the energies of low-angular-momentum states relative to high-angular-momentum states, one can readily deduce that relativity will, in general, tend to delay the onset of any structural phase transition that is triggered by a reordering of the electron energy bands.

Another feature of the bcc–fcc energy difference curves that can be understood through the type of analysis given above is the variation of the relativistic correction with volume; see figure 2. At zero pressure, the relativistic correction is quite small. As the volume decreases, however, the correction steadily increases, reaching a maximum at a relative volume near 0.5,

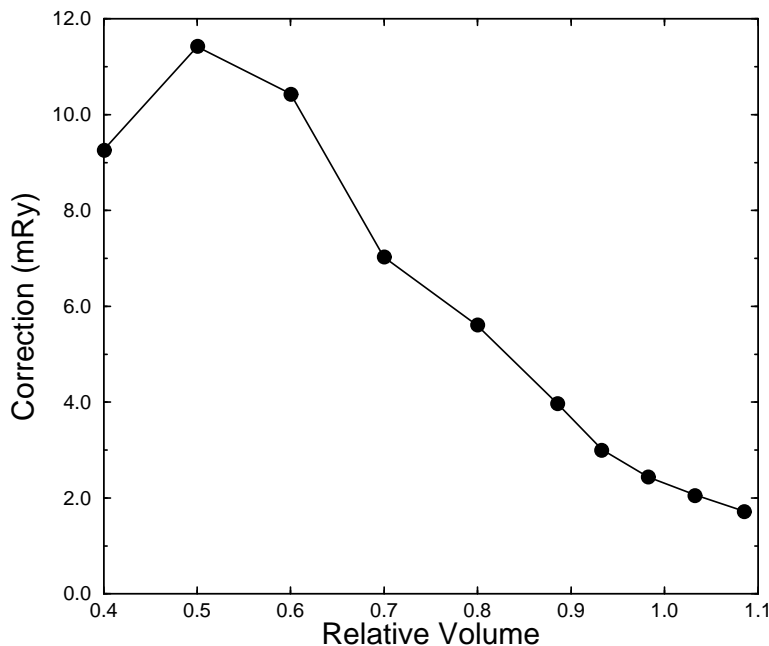


Figure 2. The negative of the relativistic correction to the bcc–fcc structural energy difference of Mo is shown as a function of the relative volume. The reference volume is 104.951 au.

at which point it begins to decrease. It is known that under pressure the initially fully occupied 5s band of Mo is driven through the partially occupied 4d band [15]. Thus, under pressure, Mo transforms from a d-bonded material (relatively insensitive to relativistic effects) to a mixed s- and d-bonded material (with significant relativistic effects) and then eventually returns to being a d-bonded material (with small relativistic effects). This analysis suggests that relativity can play an important role in the high pressure properties of materials that are unaffected by relativity at low pressures.

The bcc \rightarrow fcc transition pressure for Mo was obtained both relativistically and non-relativistically by fitting the cohesive energies for the nine largest volumes in table 1 with the modified universal equation of state and finding the point at which the enthalpy versus pressure curves for the two structures cross. The nonrelativistic LCGTO-FF calculations yield a bcc \rightarrow fcc transition pressure of 4.7 Mbar at a relative volume of about 0.55. The more realistic scalar-relativistic calculations produce a higher transition pressure of 6.6 Mbar at a relative volume of about 0.51. Since the bcc \rightarrow fcc transition has not been observed experimentally at this time, there are no firm data with which to compare these results.

5. Conclusions

It has been demonstrated here that the scalar-relativistic LCGTO-FF method as embodied in the program GTOFF produces zero-pressure properties of Mo that are nearly indistinguishable from the results of other scalar-relativistic calculations. More importantly, it has been shown that the LCGTO-FF technique is able to resolve a particularly delicate relativistic effect—namely, the volume-dependent correction to the bcc–fcc structural energy difference. It is argued that relativity will tend to delay structural phase transitions that are triggered by

pressure-induced reordering of electronic states. The current results also suggest that relativity must be taken into consideration when studying the high-pressure properties of materials even if they are unaffected by relativity at low pressures, since pressure can alter the basic nature of the bonding. Contrary to previous theoretical work, the present investigation finds no region of hcp stability at $T = 0$. Instead, the bcc structure is found to transform directly to the fcc structure at a pressure of 6.6 Mbar, for a relative volume of about 0.51.

Acknowledgments

I thank P Söderlind for helpful communications and for carrying out a series of FLMTO calculations testing the effect of f-type basis functions on the hcp–fcc structural phase stability of Mo. This research was supported by the US Department of Energy under contract W-7405-ENG-36.

References

- [1] Kutzelnigg W 1984 *Int. J. Quantum Chem.* **25** 107
- [2] Douglas M and Kroll N M 1974 *Ann. Phys., NY* **82** 89
- [3] Hess B A 1986 *Phys. Rev. A* **33** 3742
- [4] Jansen G and Hess B A 1989 *Phys. Rev. A* **39** 6016
- [5] Rösch N and Häberlen O D 1992 *J. Chem. Phys.* **96** 6322
Häberlen O D and Rösch N 1992 *Chem. Phys. Lett.* **199** 491
Häberlen O D 1993 *PhD Thesis* Technische Universität München
- [6] Geipel N J M and Hess B A 1997 *Chem. Phys. Lett.* **273** 62
- [7] Dovesi R, Pisani C, Roetti C, Causà M and Saunders V R 1989 *CRYSTAL88 (QCPE No 577)* Bloomington, IN
Pisani C, Dovesi R and Roetti C 1988 *Springer Lecture Notes In Chemistry* vol 48 (Berlin: Springer)
- [8] Boettger J C 1998 *Phys. Rev. B* **57** 8743
- [9] Boettger J C 1993 *Int. J. Quantum Chem. Symp.* **27** 147
Boettger J C and Trickey S B 1985 *Phys. Rev. B* **32** 1356
Mintmire J W, Sabin J R and Trickey S B 1982 *Phys. Rev. B* **26** 1743
- [10] Birkenheuer U, Boettger J C and Rösch N 1994 *J. Chem. Phys.* **100** 6826
Birkenheuer U 1994 *Dissertation* TU München
- [11] Boettger J C 1995 *Int. J. Quantum Chem. Symp.* **29** 197
- [12] Moruzzi V L, Janak J F and Williams A R 1978 *Calculated Electronic Properties of Metals* (New York: Pergamon)
- [13] Mattheiss L F and Hamann D R 1986 *Phys. Rev. B* **33** 823
- [14] Alouani M, Albers R C and Methfessel M 1991 *Phys. Rev. B* **43** 6500
- [15] Moriarty J A 1992 *Phys. Rev. B* **45** 2004
- [16] Sigalas M, Papaconstantopoulos D A and Bacalis N C 1992 *Phys. Rev. B* **45** 5777
- [17] Ozoliņš V and Körling M 1993 *Phys. Rev. B* **48** 18 304
- [18] Vitos L, Kollár J and Skriver H L 1997 *Phys. Rev. B* **55** 13 521
- [19] Söderlind P, Eriksson O, Johansson B and Wills J M 1994 *Phys. Rev. B* **49** 2004
- [20] Some preliminary results from this investigation were presented at the 1998 Sanibel Symposium:
Boettger J C 1998 *Int. J. Quantum Chem.* **70** 825
- [21] Ramana M V and Rajagopal A K 1983 *Adv. Chem. Phys.* **54** 231
- [22] Foldy L L and Wouthuysen S A 1950 *Phys. Rev.* **78** 29
- [23] Boettger J C 1997 *Int. J. Quantum Chem.* **65** 565
- [24] Hess B A, Buenker R J and Chandra P 1986 *Int. J. Quantum Chem.* **29** 737
- [25] Hedin L and Lundqvist B I 1971 *J. Phys. C: Solid State Phys.* **4** 2064
- [26] Dunlap B I, Connolly J W D and Sabin J R 1979 *J. Chem. Phys.* **71** 3396
- [27] Huzinaga S 1977 *J. Chem. Phys.* **66** 4245
- [28] Banerjee A and Smith J R 1988 *Phys. Rev. B* **37** 6632
For the exact form used here, see
Boettger J C and Trickey S B 1996 *Phys. Rev. B* **53** 3007
- [29] Katahara K W, Manghnani M H and Fisher E S 1979 *J. Phys. F: Met. Phys.* **9** 773

- [30] The 20 K lattice constant was obtained with data from
Touloukian Y S, Kirby R K, Taylor R E and Desai P D (ed) 1977 *Thermal Expansion: Metallic Elements and Alloys (Thermophysical Properties of Matter vol 12)* (New York: Plenum) p 208
- [31] Söderlind P 1998 unpublished
- [32] McMahan A K and Moriarty J A 1983 *Phys. Rev. B* **27** 3235